ELSEVIER

Journal of Fluids and Structures 21 (2005) 689–705

JOURNAL OF FLUIDS AND STRUCTURES

www.elsevier.com/locate/jfs

The effect of fins on vortex shedding from a cylinder in cross-flow

S. Ziada[a,*], D. Jebodhsingh[a], D.S. Weaver[a], F.L. Eisinger[b]

[a]*Mechanical Engineering, McMaster University, Hamilton, Ont, Canada, L8S 4L7*
[b]*Foster Wheeler Corporation, Clinton, New Jersey, USA*

Received 10 September 2004; accepted 3 December 2004

Abstract

A bare tube and three segmented-finned tubes have been tested to investigate the effect of the fins on vortex shedding from cylinders in cross-flow. The addition of the fins is found to enhance the process of vortex shedding. It is shown that the fins increase the correlation length and the amplitude of velocity fluctuation at the vortex shedding frequency. The fins also increase the nonlinear nature of the flow in the wake, as evidenced by a remarkable increase in the number and in the amplitude of the higher harmonic components of vortex shedding. However, the correlation length in the wake of the finned tubes is found to change with angular rotation of the tube around its axis. This phenomenon seems to be related to an irregular wavy pattern of the fin distribution along the tube axis.

1. Introduction

The phenomenon of vortex shedding in the wake of isolated cylinders and inside tube arrays exposed to cross-flow has been investigated extensively, because it can cause large amplitude resonant vibrations or generate intolerable noise levels (Bloor and Gerrard, 1966; Blevins, 1984, 1994; Weaver, 1993; Oengören and Ziada, 1998; Ziada and Oengören, 1992, 2000). The majority of previous work dealt with bare tubes and very little attention has been given to finned tubes although various types of the latter are widely used in industrial applications such as air heaters, gas coolers and boilers (Reid and Taborek, 1994). Intuitively, if the fins were to be considered as "vortex spoilers", or generators of streamwise vorticity, they ought to disturb the shed vortices, making them less coherent and three dimensional, and thereby weaken their effect as an excitation source [see for example Zdravkovich (1981)]. However, several studies of vortex shedding from finned tubes do not seem to support such expectations. For example, Mair et al. (1975) reported that vortex shedding still occurs in the wake of finned tubes and found the shedding frequency to be correlated relatively well with the tube effective diameter, which is based on the projected frontal area of the cylinder. More recently, similar features were observed by Hamakawa et al. (2001). They found the spanwise scale of the wake vortices to be considerably larger than the pitch of the fins. Vortex-induced resonant vibration of a finned tube in water cross-flow has also been reported by Katinas et al. (1991).

For the case of finned tube arrays, conflicting results have been reported. While Kouba (1986) and Nemoto and Yamada (1992, 1994) suggested that the fins had no noticeable effect on the generation of noise in finned tube arrays,

*Corresponding author. Tel.: +1 905 525 9140x27530; fax: +1 905 572 7944.
E-mail address: ziadas@mcmaster.ca (S. Ziada).

0889-9746/$ - see front matter © 2005 Elsevier Ltd. All rights reserved.
doi:10.1016/j.jfluidstructs.2004.12.003

Nomenclature

D	bare tube diameter (m)	U_o	freestream velocity (m/s)
L	tube length (m)	f_v	vortex shedding frequency (Hz)
D_e	effective tube diameter (m)	s	fin spacing (m)
D_f	fin diameter (m)	t	fin thickness (m)
Re	Reynolds number based on D	$\acute{u}$	local r.m.s. fluctuating velocity (m/s)
$R_{uu}(z)$	correlation coefficient based on fluctuating velocity measurements	x	streamwise coordinate (m)
		y	transverse coordinate (m)
		z	axial coordinate (m)
St_{De}	Strouhal number based on D_e	λ_z	correlation length (m)

Nemoto et al. (1997) found the acoustic resonance of finned tube arrays to be much stronger than that occurring in bare tube arrays. The increase in the sound pressure level due to the fins was as high as 20–30 dB. These contradictions are not surprising since the fins are expected to influence not only the shedding phenomenon, but also sound attenuation (or acoustic damping) due to viscous losses between the fins. Both of these effects are expected to be dependent on the fin pitch and height as well as on the spacing ratios between the tubes.

The above findings indicate clearly that coherent vortex shedding can occur in the wake of an isolated finned cylinder as well as inside arrays fabricated of finned tubes. However, several unresolved issues still need to be investigated in order to improve our fundamental understanding of the effect of fin geometry on the mechanisms of sound generation and vortex-induced vibration of finned tubes. For example, it is not clear how the fins affect the streamwise development of the wake profile of turbulence intensity, or the correlation length of wake vortices. These are the basic parameters that are needed to estimate the characteristics of unsteady fluid loading and sound generation by vortex shedding from finned tubes.

This paper focuses on some of these unresolved issues for the simple case of a finned tube exposed to cross-flow. Three tubes with similar fin height but different fin density (i.e. different number of fins/unit tube length) are tested in a wind tunnel at two Reynolds numbers in the subcritical regime (2.61×10^4 and 4.98×10^4). The effect of fins is examined by comparing the wake characteristics with those of a bare tube whose diameter is the same as the root diameter of the fins. Extensive hot-wire measurements and correlation analysis are performed to delineate the effect of the fins on the streamwise evolution of the mean and fluctuating velocity profiles and on the correlation length of vortex shedding.

2. Experimental set-up

The experiments were performed in an open-circuit, subsonic wind tunnel equipped with a variable speed controller. As shown in Fig. 1(a), the test-section was octagonal in shape with the walls made of 19.05-mm-thick clear acrylic. The perpendicular distance between the flats of the section was 609.6 mm with the tube being rigidly mounted across the middle of the section. The tube was held rigidly in place by clamping between two end plates, which were supported by the vertical sides of the test section. The end-plates were used to reduce three-dimensional flow effects due to the boundary layer on the tunnel wall and were designed based on the findings of Stansby (1974) and Szepessy and Bearman (1992). They were rectangular in shape (254×355 mm), made of 4.8-mm-thick clear acrylic and were located 25.4 mm away from the tunnel wall to ensure that they were outside the boundary layer.

Four tubes were selected for testing of which three were segmented-finned tubes of different fin densities but same fin height, and the fourth was a bare tube, which was considered to be a baseline against which the finned tubes could be compared. The finned tubes were actual full-sized tubes used in heat recovery steam generators. They were made of steel, with the segmented fins being helically wound along the axis of the tube. The diameter of the baseline bare tube was the same as the root diameter of the fins. Additional specifications of the tested tubes can be found in Table 1.

In this study, an effective diameter, D_e, is used for the finned tubes. As fins are added to a bare tube of diameter D, the effective diameter becomes larger than D, but still less than the outer fin diameter, D_f. Estimation of the effective diameter is based on the increase in flow blockage caused by the fins, rather than the increase in tube volume. The values of D_e given in Table 1 are calculated from the following formula proposed by Mair et al. (1975):

$$D_e = (1/s)\{(s-t)D + tD_f\}. \tag{1}$$

As shown in Fig. 1(b), s is the fin spacing (or pitch) and t the fin thickness.

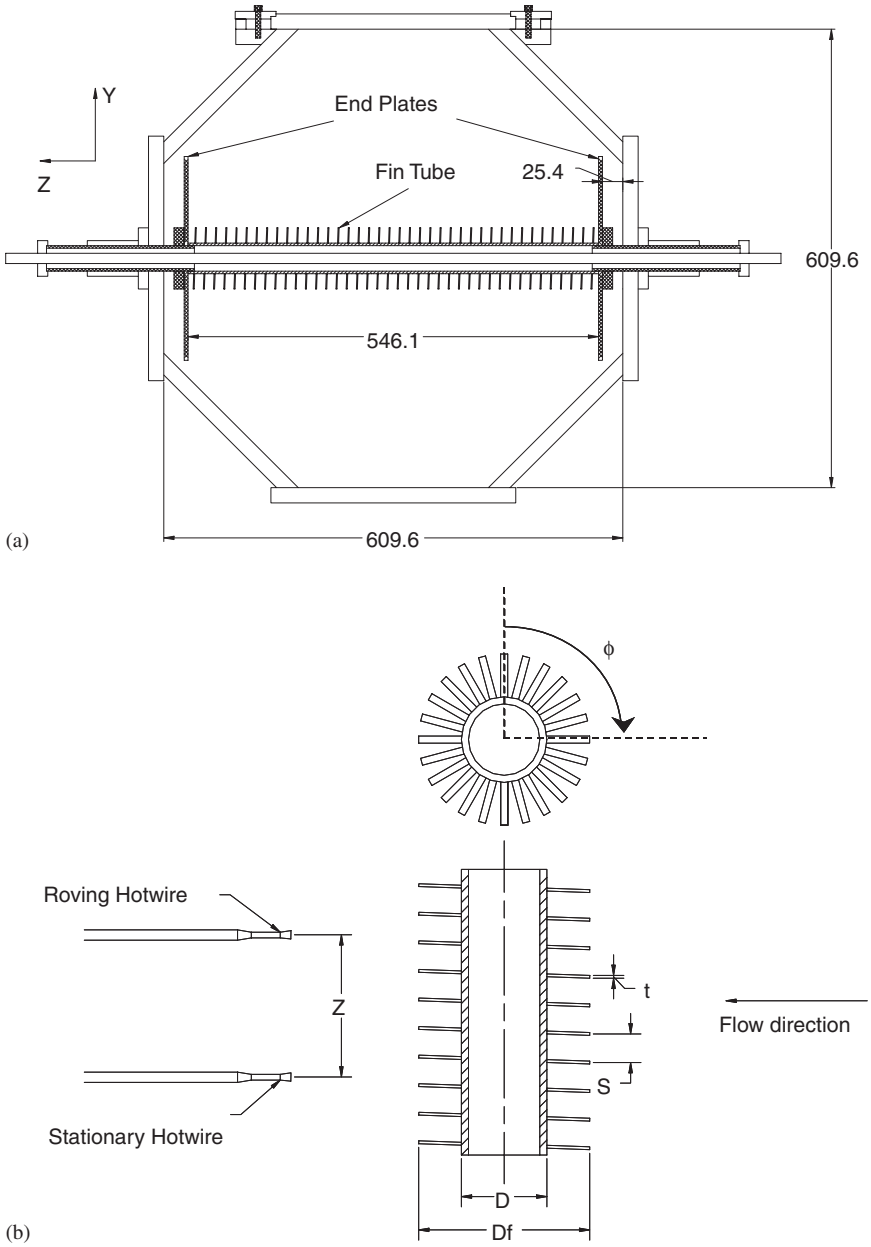

Fig. 1. Test set-up showing (a) the finned tube and end plates (all dimensions in mm) and (b) details of fin geometry and the method used to measure the spanwise correlation coefficient of the velocity fluctuation.

All measurements taken throughout this investigation were obtained by two hot-wires, type Dantec 55P11, operated by two Dantec 55M10 CTA Standard Bridges. The signals of the hot-wires were digitized using a National Instruments PCI-6024E, 8 channel, 12 bit, simultaneous sampling data acquisition system. The data was collected using a real-time Labview program, which was able to display and record time signals, power spectrum of fluctuating velocity for each channel, as well as the correlation coefficient between the two hot-wire signals. As velocity measurements were required at various spatial positions, a computer controlled, three-axis traversing mechanism was employed to position the hot-wires.

All experiments were performed at two Reynolds numbers, $\mathrm{Re} = 2.61 \times 10^4$ and 4.98×10^4 (referred to hereafter as low or high Re case, respectively), and at two distances downstream of the tube center ($2.5D_e$ and $5D_e$). Obtaining wake profiles involved the use of one hot-wire at a particular downstream distance, which was traversed across the wake and

Table 1
Physical specifications of the tested tubes (dimensions in millimeters)

	Bare tube	Finned tube 1	Finned tube 2	Finned tube 3
Length, L	546.1	546.1	546.1	546.1
Bare tube diameter, D	38.1	38.1	38.1	38.1
Fin thickness, t	—	1.27	1.27	1.27
Fin density (fins/inch)	—	3.5	5	7
Fin height	—	19.05	19.05	19.05
Fin spacing, s	—	7.26	5.08	3.63
Outer fin diameter, D_f	—	76.2	76.2	76.2
Effective diameter, D_e	38.1	44.8	47.6	51.4
Blockage ratio (%)	6.76	7.94	8.45	9.12

measurements were taken at various points. It should be noted that due to physical constraints, fewer measurements were taken on one side of the wake, which will be clearly seen in the wake profile results. Measurement of correlation length required both hot-wire probes. They were first placed together, as close as physically possible, at a particular downstream distance, and then one hot-wire was moved away from the stationary wire in the axial direction (z), and the correlation coefficient between the signals ($R_{uu}(z)$) was measured as a function of the separation distance (z). Fig. 1(b) illustrates this process. The correlation coefficient $R_{uu}(z)$ was plotted against separation distance (z) with the area under the graph giving the correlation length, λ_z.

3. Spectral content of velocity fluctuation

Fig. 2 shows typical spectra of the velocity fluctuations for each tube as the hot-wire was traversed from the center of the wake ($y/D_e = 0$) to the free stream. All spectra were taken at a streamwise location of $x/D_e = 2.5$. The root-mean-square (r.m.s.) amplitude of velocity fluctuation u' is normalized by the free stream velocity U_o, and the frequency f is expressed in terms of Strouhal number, $\mathrm{St}_{De} = fD_e/U_o$, which is based on the effective tube diameter. From these spectra, it is seen that vortex shedding peak, f_v, occurs at $\mathrm{St}_{De} \approx 0.2$.

The most significant difference seen between the spectra of the four tubes is the appearance of numerous higher harmonic components of vortex shedding when the fins are added. The number of these components appears to increase as the fin density is increased. For example, outside the wake region, $y/D_e > 1.5$, the spectra of the bare tube hardly show any harmonic components, whereas those of the finned tubes clearly depict the presence of at least two harmonics ($2f_v$ and $3f_v$, where f_v is the vortex shedding frequency). As the wake center-line is approached, the bare tube spectra show a couple of harmonics, but as many as eight harmonics can be seen in the spectra of finned tubes. The enhancement of the harmonic components of vortex shedding by the fins is further delineated in Fig. 3, which compares velocity spectra for the four tubes measured at comparable locations in their wakes, for the high Reynolds number case. Increasing the fin density is seen to drastically enhance the generation of the vortex shedding higher harmonics.

The generation of higher harmonics in free shear flows, such as the present wake, is an inherent feature of their instability mechanism. Nonlinear stability analysis (Stuart, 1971; Robinson, 1974; Benney and Bergeron, 1969) shows that when the amplitude of disturbance exceeds a certain value ($u'/U_o \approx 3\%$), it is necessary to consider viscous and/or nonlinear terms in the governing vorticity equation, which leads to the generation of higher harmonics of the fundamental frequency of oscillation. Ziada and Rockwell (1982), for example, found the measured growth rates of these harmonics to agree rather well with those predicted from the nonlinear stability theory. Thus, for the present case, the enhancement of the higher harmonics of vortex shedding due to the addition of fins may be attributed to the increase in the amplitude of velocity fluctuation and/or to the introduction of three-dimensional disturbances by the fins. In fact, as will be discussed later, the amplitude of velocity fluctuations in the finned tube wakes is found to be substantially larger than that observed in the bare tube wake. Therefore, the enhancement of harmonics seems to be caused primarily by the increase in velocity fluctuations. The effect of three-dimensional disturbances seems to be of less importance, since their wavelength is much smaller than that of vortex shedding (Benney and Bergeron, 1969). Moreover, the presence of spanwise structure is not a necessary condition for generation of higher harmonics.

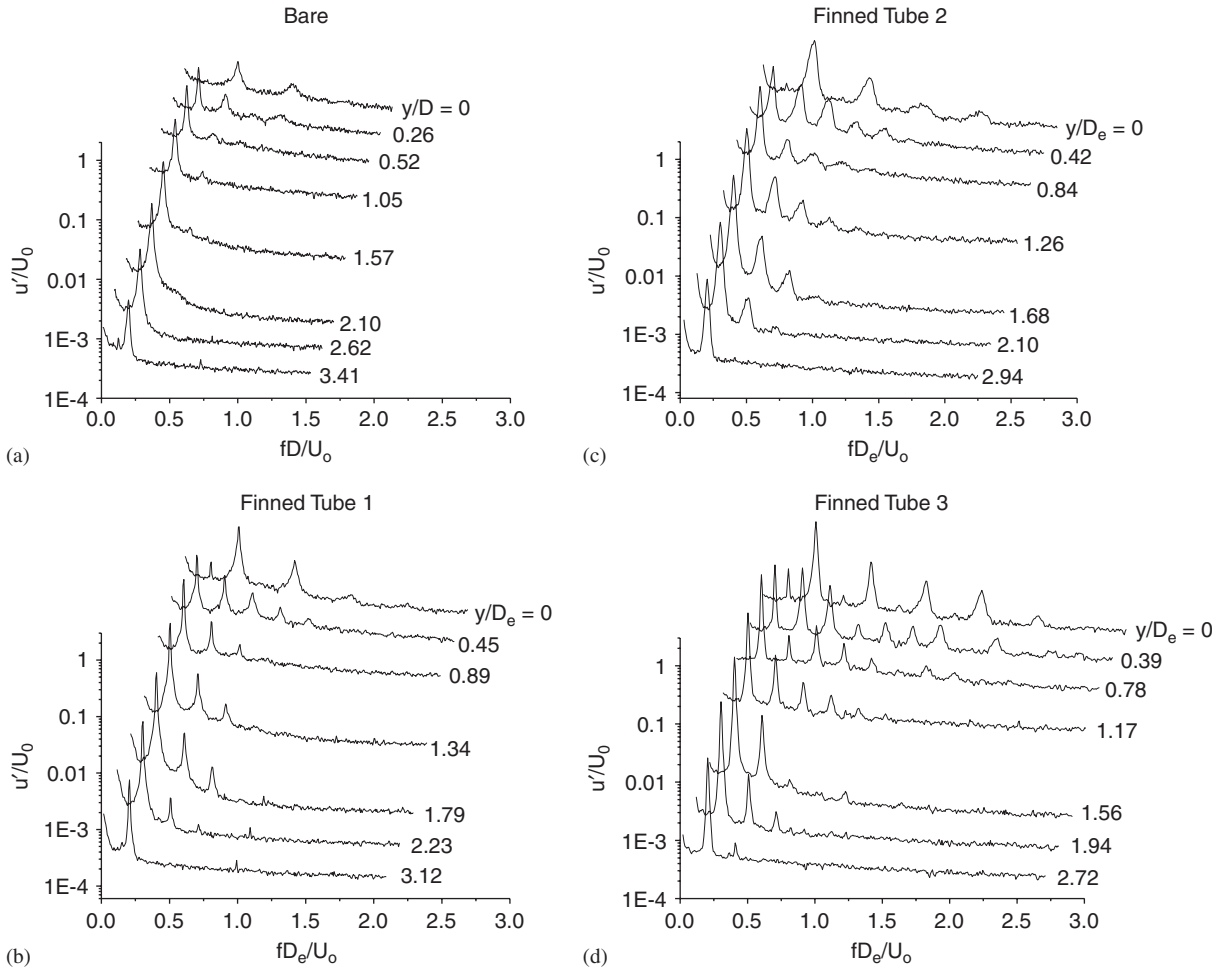

Fig. 2. Typical spectra of velocity fluctuations measured at various transverse locations. $x/D_e = 2.5$; high Reynolds number case.

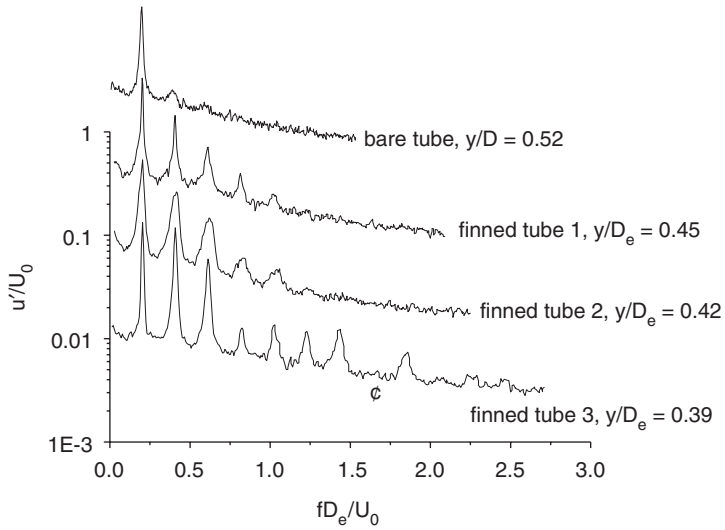

Fig. 3. Spectra of velocity fluctuations for the bare and finned tubes measured at $x/D_e = 2.5$ and comparable y/D_e locations. High Reynolds number case.

As the measurement location moves towards the wake center-line, all frequency components, including the fundamental frequency, are seen to first increase in magnitude, but then closer to the center-line, the fundamental frequency as well as its odd harmonics ($f_v, 3f_v, 5f_v, \ldots$) start to decrease in magnitude until the wake center-line is reached where these peaks virtually disappear. Simultaneously, as those frequencies decrease, the odd harmonic frequency peaks ($2f_v, 4f_v, \ldots$) increase in magnitude.

Mair et al. (1975) noticed that fins tend to increase the sharpness of the vortex shedding peak in the turbulence spectra and postulated that the fins, which were made of *solid* discs oriented normal to the tube axis, have increased the two-dimensionality of the flow. Such a trend does occur for the present tubes with *spirally wound segmented* fins, except for finned tube 2, for which the peaks are obviously not as sharp as for any of the other tubes. From these spectra, it can also be seen that the vortex shedding peak and its harmonics become larger in magnitude as the fin density increases.

Since the fins introduce streamwise vorticity and three-dimensional disturbances, they have some similarities with classical means of suppressing vortex shedding (Zdravkovich, 1981) and as such, they might be expected to weaken the vortex shedding process. Surprisingly, vortex shedding does occur for finned tubes and in fact seems to be strengthened with the addition of fins.

4. Mean velocity profiles

The mean velocity profile was measured at several locations and at the selected cases of Reynolds number. Typical profiles measured at $x/D_e = 2.5$ and 5 for the low Reynolds number case are shown in Fig. 4. The profiles for finned tubes 1 and 2 are very similar in shape to that of the bare tube with the exception that the fins produce a much larger velocity deficit. As noted earlier, D_e is used as the characteristic dimension for the finned tubes and therefore, the location of the profile measurement is further downstream for the finned tubes and the transverse coordinate is normalized with a larger D_e as the fin density increases. Although using the effective diameter as length scale seems to account for the differences in wake width of all tubes, it is clearly not adequate to explain the large differences in the velocity deficit. Even though the measurements were taken further downstream for the finned tubes, the velocity deficits for finned tubes 1 and 2 are still larger than that for the bare tube.

The most striking feature of this figure is the profile for finned tube 3. Its shape is unlike that of any of the other tubes. At $x/D_e = 2.5$, Fig. 4(a), as the tube axis is approached, the mean velocity first decreases, then increases, and finally decreases once more until the maximum velocity deficit is reached at the wake center-line. Note that the wake profile is still almost symmetric at this location. Further downstream, as shown in Fig. 4(b) for $x/D_e = 5$, the wake symmetry is entirely lost and, in fact, the mean velocity in the wake left-hand side is higher than the approach flow velocity. This dramatic change in velocity profile for the highest fin density suggests that there may be a transition boundary related to fin density beyond which a significant change occurs in the behaviour of flow over the finned tubes.

In order to shed more light on these unusual profiles for finned tube 3, additional measurements were made at several downstream locations and the results are shown in Fig. 5. At $x/D_e = 1.5$ the profile looks similar to what would be expected with a symmetric velocity deficit aligned with the wake center-line. At $x/D_e = 2.5$ and larger, the deviation from the wake of the bare tube becomes progressively stronger including loss of symmetry. It is remarkable how fast the

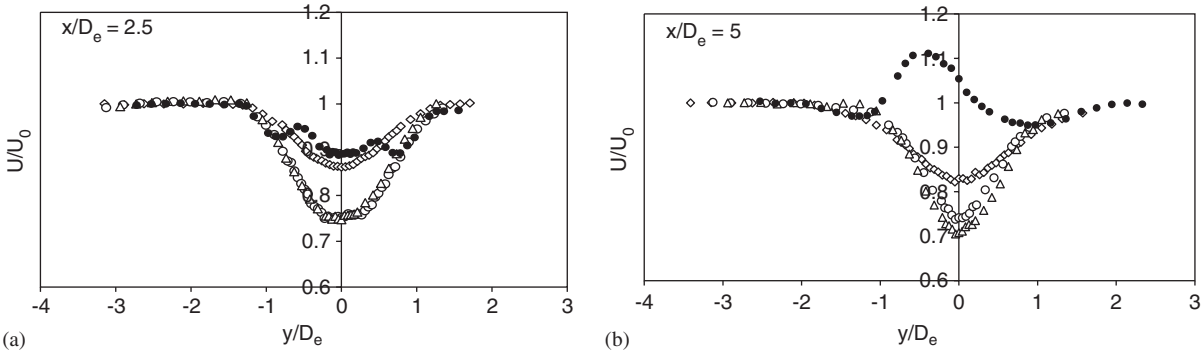

Fig. 4. Wake profiles of normalized mean velocity for all tubes for the low Reynolds number case. (a) $x/D_e = 2.5$; (b) $x/D_e = 5$; ◇, bare tube; ○, finned tube 1; △, finned tube 2; ●, finned tube 3.

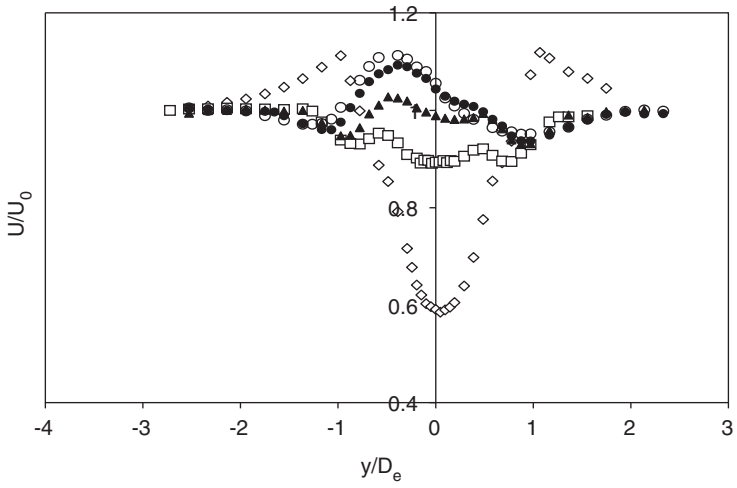

Fig. 5. Wake profiles of normalized mean velocity at various downstream distances for finned tube 3 at the low Reynolds number. ◇, $x/D_e = 1.5$; □, 2.5; ▲, 3; ●, 4; ○, 5.

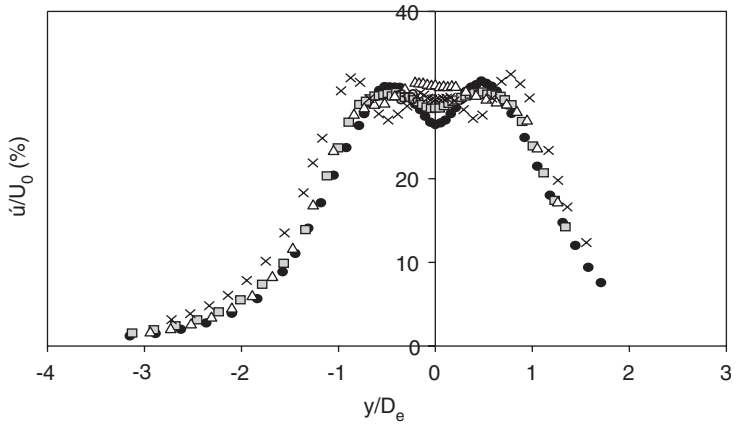

Fig. 6. Profiles of total streamwise turbulence intensity. $x/D_e = 2.5$; low Reynolds number case; ●, bare tube; □, finned tube 1; △, finned tube 2; x, finned tube 3.

wake velocity profile is recovered to an "almost uniform profile" at $x/D_e = 3$. Further downstream, profiles similar to that shown in Fig. 4 start to develop.

Despite these unusual features of the mean velocity profiles for finned tube 3, the profiles of the velocity fluctuations, which are discussed in the next section, exhibit remarkable symmetry about the wake center-line. The flow mechanisms causing these features are not yet understood, but are currently being investigated.

5. Profiles of fluctuating velocity

Fig. 6 shows typical profiles of turbulence intensity, normalized by U_o, for all tubes measured at $x/D_e = 2.5$. The turbulence intensity here refers to the total r.m.s. amplitude of streamwise velocity fluctuations, which is represented by the area under frequency spectra such as those in Fig. 3. The turbulence profiles show a gradual transition with increased fin density, from the bare tube to finned tube 3. The profile of finned tube 1 is very similar to the bare tube profile, with the exception of exhibiting a smaller turbulence intensity deficit at the wake center-line. For finned tube 2,

there is only a very slight deficit in the turbulence profile. The turbulence intensity profile for finned tube 3 depicts a hump at its center and two deficits near $y = \pm 0.45 D_e$. Since the turbulence intensity is related to the frequency spectra, the amplitudes of the higher harmonics, which are largest at the center, are expected to strongly influence the amount of deficit in the turbulence intensity profile. From Fig. 6, it could then be inferred that increasing the fin density increases the strength and number of higher harmonics; thus giving rise to more complex profile shapes near the wake center-line.

It should be pointed out that using the effective diameter to normalize the transverse coordinate, y, improves the collapse of all turbulence profiles, especially those of the bare and finned tubes 1 and 2. Moreover, the maximum turbulence intensity is approximately the same for all tubes, between 30% and 32%. Thus, the *total* energy level of velocity fluctuations in the wake of every finned tube appears to be comparable with that of the bare tube. Measurements at different locations and Reynolds numbers showed similar features and can be found in Jebodhsingh (2002).

Fig. 7 shows the r.m.s amplitude of the velocity fluctuation at the vortex shedding frequency, $\acute{u}(f_v)$, which constitutes the contribution of the fundamental component to the total turbulence intensity.

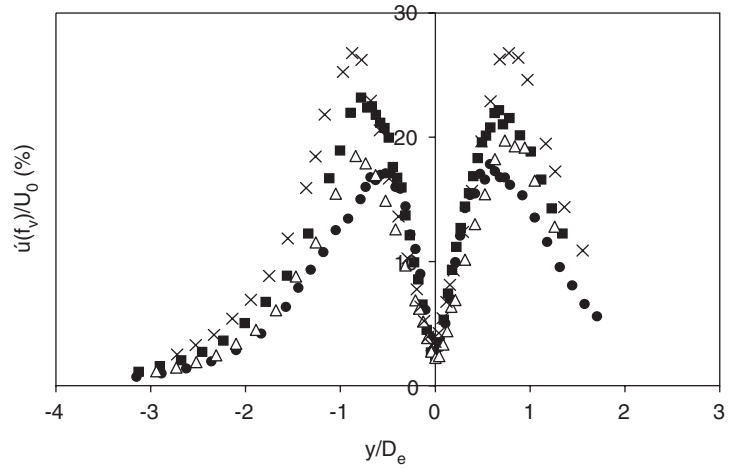

Fig. 7. Amplitude of velocity fluctuations, $\acute{u}$, at the vortex shedding frequency, f_v, showing the contribution of the fundamental component, $\acute{u}(f_v)$, to the total turbulence intensity. $x/D_e = 2.5$; low Reynolds number case; ●, bare tube; ■, finned tube 1; △, finned tube 2; x, finned tube 3.

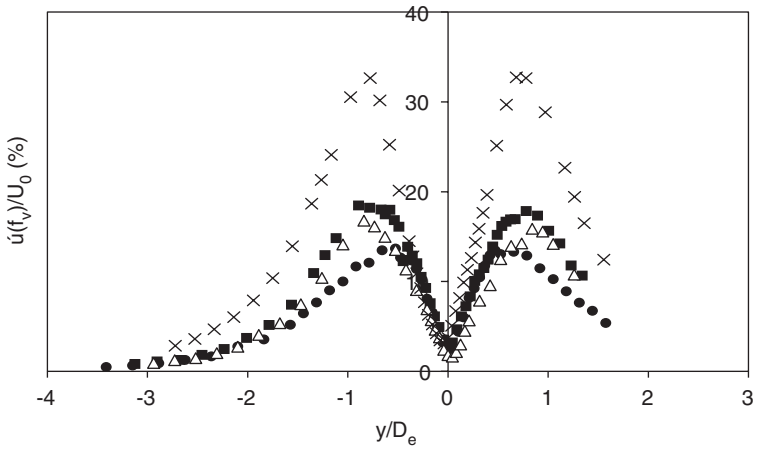

Fig. 8. Amplitude of velocity fluctuations, $\acute{u}$, at the vortex shedding frequency, f_v, showing the contribution of the fundamental component, $\acute{u}(f_v)$, to the total turbulence intensity. $x/D_e = 2.5$; high Reynolds number case; ●, bare tube; ■, finned tube 1; △, finned tube 2; x, finned tube 3.

The fins have the effect of increasing the amplitude of the velocity fluctuation. Finned tube 3, with the highest fin density, generates the largest velocity fluctuation, which is about 50% higher than that of the bare tube. For all cases, the bare tube has the smallest amplitude of velocity fluctuation. However, the results do not show a progression in the amplitude of vortex shedding peak with increased fin density. This lack of progression may be attributed to variations in the width of the vortex shedding peak, as can be seen for finned tube 2 in Fig. 2. Only for the low Re case and at $x/D_e = 5$ (not shown) does the trend of increased peak height with fin density occur.

One of the more interesting features is that the fundamental frequency of vortex shedding accounts for a large portion of the total turbulence intensity away from the wake center-line. Also, the fundamental frequency component is seen to contribute a significantly larger portion to the overall turbulence for tubes with fins. For instance, at the peak values of this particular case, the fundamental frequency component accounts for about 82% of total turbulence intensity of finned tube 3, but only 54% for the bare tube case. The most striking difference between bare and finned tubes is seen at high Re and $x/D_e = 2.5$, which is illustrated in Fig. 8. The velocity fluctuation amplitude of finned tube 3 is 2.5 times higher than that of the bare tube. All these results indicate that, although the fins do not increase the total turbulence intensity in the wake, they do concentrate the fluctuating energy of the flow at the vortex shedding frequency and its higher harmonics. In other words, vortex shedding from the tested finned tubes must be more intense and organized than that occurring in the bare tube wake.

The results of the first harmonic of vortex shedding show trends similar to those of the fundamental component, as illustrated in Fig. 9. The fins increase the amplitude of the first harmonic component. This amplitude decreases when the Reynolds number and/or downstream distance are increased. Again, the first harmonic amplitude is always the largest for finned tube 3, while the bare tube has the smallest amplitude. Note that the profiles of all cases are almost symmetric. As mentioned earlier, higher amplitude harmonics are generated when the fundamental component is stronger. The only difference in the trends between Figs. 7 and 9 is the general shape of the profiles. The amplitude profiles of the fundamental frequency are seen to increase to a maximum then decrease to a minimum at the wake center-line, while those of the first harmonic increase to a maximum at the wake center-line. Also, while the fundamental frequency profiles are seen to have similar shapes, the first harmonic profiles are seen to change with increased fin density. In addition to a peak at $y/D_e = 0$ for the finned tubes, another peak is observed at around $y/D_e = \pm 1$, and becomes more prominent with increased Reynolds number. These second peaks are barely detectable for the bare tube. Once again, the profile for finned tube 3 differs. At $x/D_e = 5$, which is not shown here but can be found in Jebodhsingh (2002), while all other tubes show a barely detectable second peak, finned tube 3 exhibits a clear second peak, but only at $y/D_e = -1$ which results in asymmetric profile.

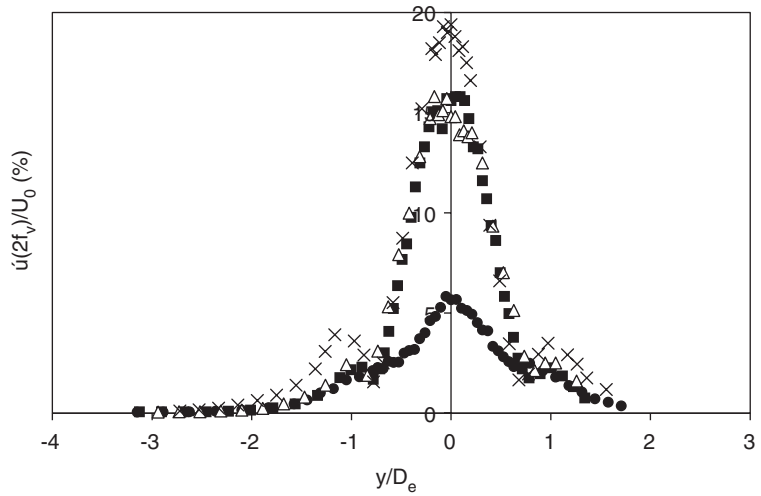

Fig. 9. Amplitude of velocity fluctuations, $\acute{u}$, at the higher harmonic of vortex shedding frequency, $2f_v$, showing the contribution of the first harmonic component, $\acute{u}(2f_v)$, to the total turbulence intensity. $x/D_e = 2.5$; low Reynolds number case; ●, bare tube; ■, finned tube 1; △, finned tube 2; x, finned tube 3.

6. Strouhal number

Similar to the bare tube case, the frequency of vortex shedding increases linearly with velocity, following a constant Strouhal number relationship. As can be seen in Fig. 10, for the same flow velocity, the addition of fins has the effect of reducing the vortex shedding frequency. This is expected since the addition of fins increases the effective diameter of the tube, which results in a decrease in the shedding frequency according to the Strouhal relationship. The Strouhal numbers assigned to each tube are estimated by fitting straight lines through the data-points, using the least mean square method. It decreases slightly with fin density, which agrees with the Strouhal number data reported by Mair et al. (1975).

For the bare tube, the Strouhal number is slightly larger than the value reported in the literature for the Reynolds number of this study ($St \approx 0.2$). However, the present Strouhal number is an average value for a much larger range of Reynolds number (0–46 000). The Strouhal number is known to be higher than 0.2 over a portion of this range (Blevins, 1994).

The effect of Reynolds number on the Strouhal number is shown in Fig. 11 for all tubes. The effective diameter D_e suggested by Mair et al. (1975) is used to calculate the Strouhal number. If D_e were to account properly for the effective

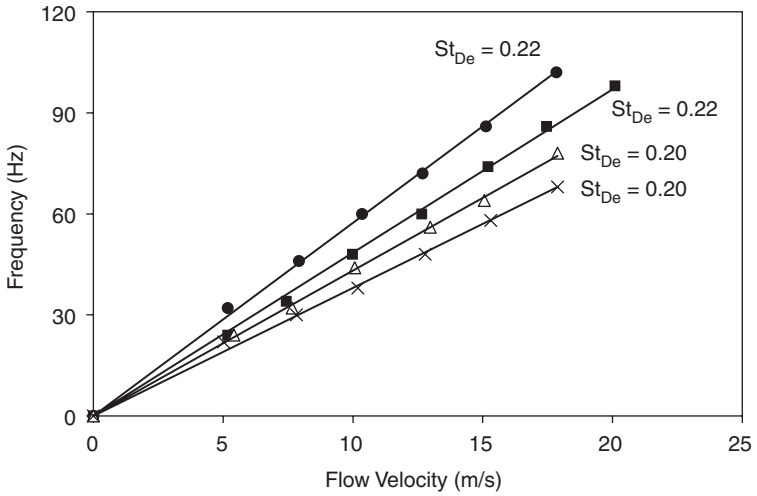

Fig. 10. Vortex shedding frequency as a function of flow velocity for all tubes. ●, bare tube; ■, finned tube 1; △, finned tube 2; x, finned tube 3.

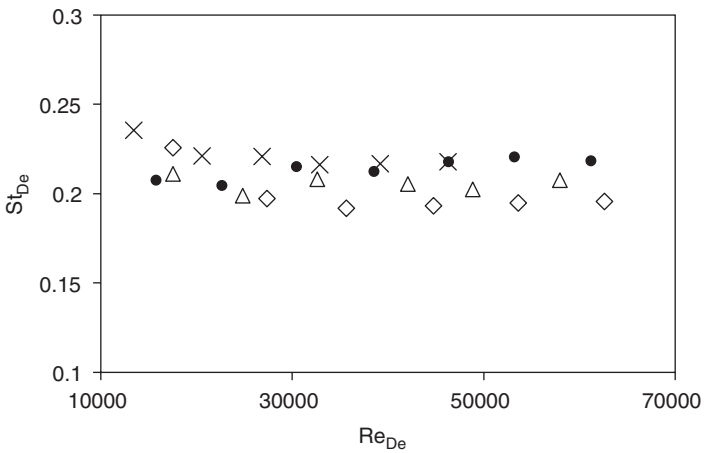

Fig. 11. Strouhal number as a function of Reynolds number for all tubes. x, bare tube; ●, finned tube 1; △, finned tube 2; ◇, finned tube 3.

increase in the tube diameter, the Strouhal number based on D_e would be the same for all finned tubes. Although D_e is found to reduce the scatter in Strouhal number data, it does not fully correlate the effect of fins on the shedding frequency. In fact, it underestimates the effect of fins, especially when the fin density is high. The reason for this deficiency is believed to be related to the effect of fins on the wake profile and momentum thickness, which are known from stability theory to be the main parameters controlling the frequency of vortex shedding.

7. Correlation length

Scrutiny of the literature related to correlation length of vortex shedding (El Baroudi, 1960; Kacker et al., 1974; Ribeiro, 1992; Szepessy and Bearman, 1992; Szepessy, 1994; Norberg, 2001) shows that there is a lack of consistency and details as to where the hot-wires were positioned in previous research. The only consistent parameter is that the hot-wires were positioned outside of the wake. For this reason, it was desired to initially explore how the correlation coefficient varies when the two hot-wires are positioned at various transverse positions (y/D_e). This was examined for three separation distances between the wires and for the bare tube and one finned tube. Since the results were similar for both cases, only the bare tube results are shown in Fig. 12.

The correlation coefficient increases as the wires move away from the wake center-line ($y/D = 0$), and reaches its maximum value at approximately the same transverse distance for the three separation distances between the wires. It was thus decided that, in order to be consistent, all measurements be taken at the transverse location corresponding to maximum correlation, which in all cases was barely outside of the wake. In this particular case, the measurements were taken at $y/D \approx 2$. However, it should be noted that this distance varied from test to test depending on the tube and Reynolds number. For example, the measurement location for the finned tubes was farther downstream and farther away from the wake center-line in comparison with the case of bare tube.

All correlation coefficients were measured at $y/D_e = 2.5$ and calculated from the following formula (Bendat and Piersol, 1980):

$$R_{xy}(0) = \frac{C_{xy}(0)}{\sqrt{C_{xx}(0)C_{yy}(0)}}, \tag{2}$$

where $x(t)$ and $y(t)$ represent the two time varying signals, C_{xy} is the cross-correlation function and C_{xx} and C_{yy} are the auto-correlation functions. In the following, the correlation coefficient will be referred to as R_{uu} to indicate that it is obtained from measurements of velocity fluctuation and not the pressure.

Fig. 13(a) shows the correlation coefficient, $R_{uu}(z)$, as a function of spanwise spacing (z) for the bare tube. These results are quite similar to those existing in the literature. At $z = 0$, R_{uu} starts close to 1 and then asymptotes to 0 with increasing z. Also, the correlation coefficient decreases with downstream distance, resulting in a smaller correlation length (λ_z). This agrees with expectation that further downstream, the vortices become weaker and less coherent due to three-dimensional effects and therefore the signals that are recorded by the two hot-wires become less correlated. It is

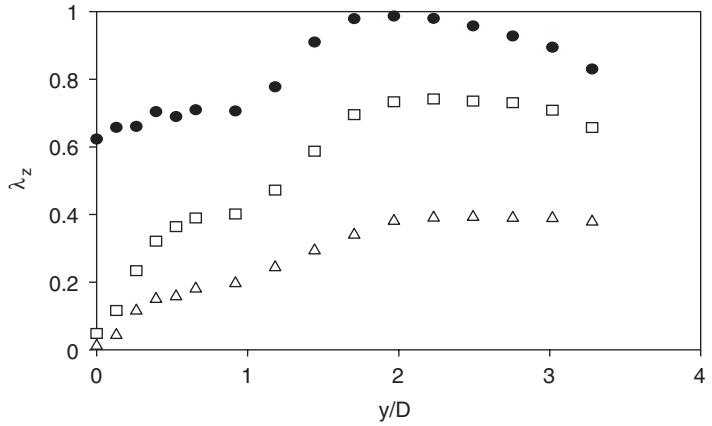

Fig. 12. Variation of correlation coefficient (λ_z) with transverse location for three different separation distances (Δz) between the hot-wires. Bare tube; $x/D = 2.5$; low Reynolds number case. ●, $\Delta z/D = 0.16$; □, $\Delta z/D = 1.99$; △, $\Delta z/D = 4.36$.

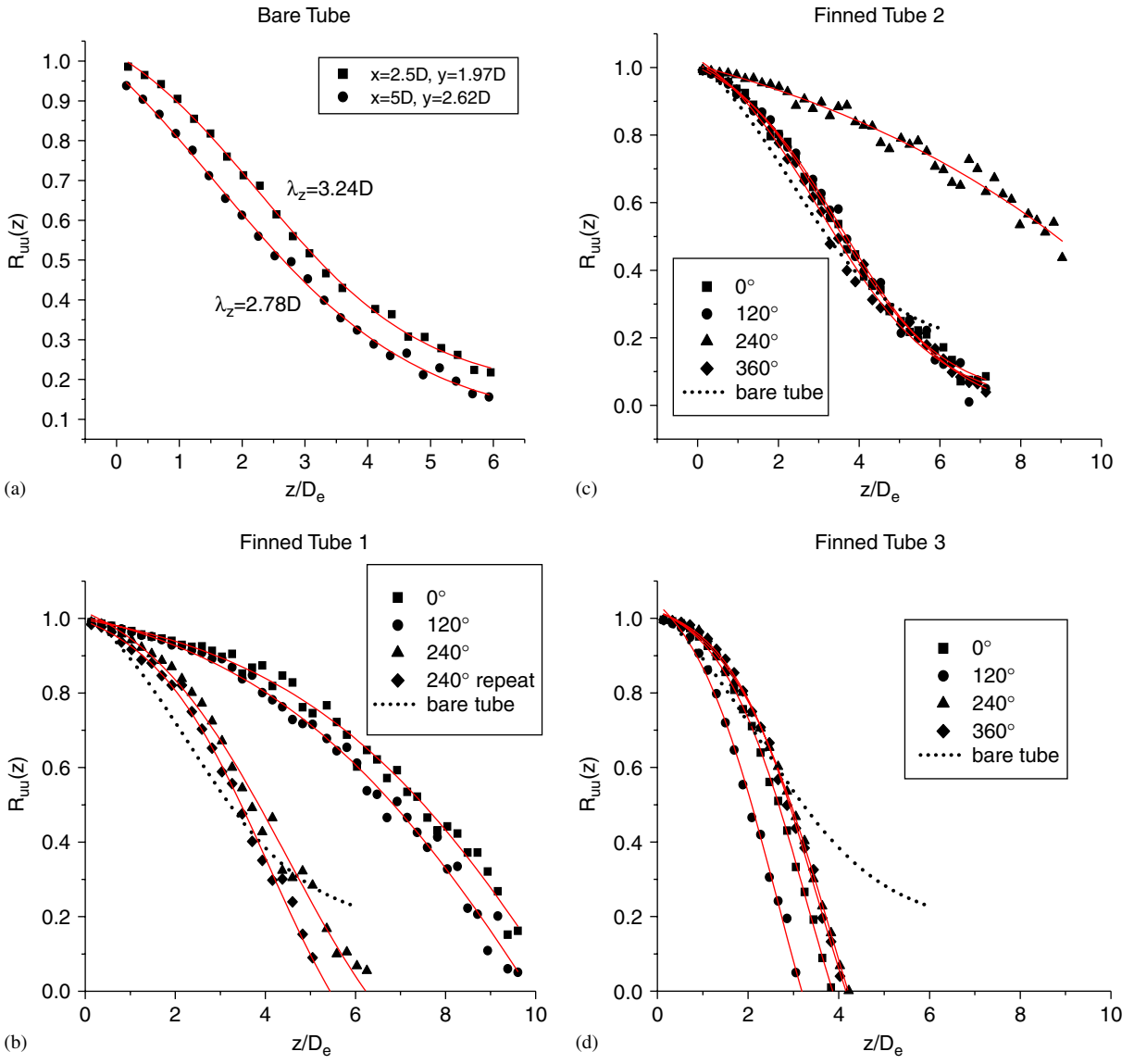

Fig. 13. Correlation coefficient along the span of all tubes at $x/D_e = 2.5$ and low Re. The results of the finned tubes are given for several angular positions.

also noted that as Reynolds number is increased, correlation length decreases slightly for both downstream distances (Jebodhsingh, 2002), which agrees with the results of Kacker et al. (1974). The values of λ_z obtained for bare tube ($\approx 3D$) agree quite well with those reported by Ribeiro (1992) for similar Reynolds number.

Correlation coefficient measurements were also performed for the finned tubes. During these tests, some of the results could not be reproduced. Repeated testing then showed that significantly different correlation coefficients are obtained if a finned tube is rotated around its axis as indicated by the angle ϕ in Fig. 1(b). Determining that the results changed considerably, it was then decided to take measurements for all finned tubes at three different angular orientations, and to repeat one orientation to ensure repeatability of the results. Thus, after measuring the correlation length at an initial orientation ($\phi = 0^\circ$), the tube was rotated around its axis by 120° and the measurements were repeated. As shown in Fig. 13, the correlation coefficient of all finned tubes is dependent on the tube rotation angle. The repeatability of the results was also confirmed because of the relatively good agreement of the results that were repeated at the same angle.

At 240° for finned tube 1, the curve of $R_{uu}(z)$ seems to follow the normal trend exhibited by the bare tube, although it asymptotes to zero more quickly. The curves for 0° and 120° are similar to each other but differ substantially from the

normal shape exhibited by the bare tube. No inflection point is seen and the values of $R_{uu}(z)$ are much larger than those at 240°, which results in almost doubling the correlation length λ_z as compared to the bare tube (see the summary in Table 2).

For finned tube 2, the results are almost identical for 0°, 120°, and 360° with these curves being very similar in shape to those of a bare tube. The curve for 240° deviates significantly from the others, showing no inflection point and appears that it would not reach $R_{uu}(z) = 0$ until well after $z/D_e = 10$. Again, the correlation length λ_z for 240° is more than twice that of the bare tube (Table 2).

The curves for finned tube 3 exhibit the least deviation when compared with each other. They follow the same trend of rapidly reaching $R_{uu}(z) = 0$ without displaying an inflection point. As shown in Table 2, the correlation lengths for all angles in this case are smaller than that of the bare tube.

Currently, the only hypothesis to possibly explain the drastic changes in λ_z with rotation angle is related to the geometry or manufacturing of the tubes. As shown in Fig. 14, looking along the axis of the tube, the fins seem to line up in a wavy pattern, which changes as the tube is rotated. The change in this pattern with rotation may influence the coherence between the velocity fluctuations along the tube span. This does not distract from the remarkable fact that, at some angles, the correlation length λ_z of finned tubes 1 and 2 is about twice that of the bare tube. Moreover, as shown in Table 2, λ_z is larger than that of the bare tube for all other angles. These results, together with the observation that the fins enhance the vortex shedding component and its higher harmonics, lead to the conclusion that vortex shedding from finned tubes may well be a stronger excitation source than that from bare tubes. These are important findings that need to be investigated further to explain the effect of tube rotation on the correlation length as well as the enhancement of the velocity fluctuations due to the addition of fins. The unusual features observed in the wake of finned tube 3, with the highest fin density, also deserve pursuing.

8. Spanwise variations in the wakes of finned tubes

The observed variability in the correlation coefficient as the finned tubes are rotated around their axes necessitated a closer look at the wake characteristics at different spanwise locations. As mentioned earlier, the fins display a wavy

Table 2
Compilation of correlation length measurements in terms of D_e recorded at $2.5D_e$ and low Reynolds number

Rotation angle, ϕ	0°	120°	240°
Finned tube 1	6.74	6.23	3.57
Finned tube 1 repeated	—	—	3.15
Finned tube 2	3.60	3.61	8.30
Finned tube 2 repeated	3.47	—	—
Finned tube 3	2.41	1.85	2.65
Finned tube 3 repeated	2.63	—	—
Bare tube		3.24	

Fig. 14. Photographs of the finned tubes showing the wavy pattern.

pattern along the tube. Additional measurements at different spanwise locations were therefore carried out to assess the effect of this pattern on the wake characteristics. The mean velocity profile and the amplitude distribution of the velocity fluctuation were measured for all finned tubes at three spanwise locations, $z/D_e \approx -2.4$, 0 and $+2.4$. These measurements were taken at $5D_e$ downstream of the finned tubes.

Fig. 15 shows three profiles of mean velocity measured at different spanwise locations for each of the finned tubes. Corresponding profiles of the amplitude of velocity fluctuation at the vortex shedding frequency, $\acute{u}(f_v)$, are given in Fig. 16. For finned tube 1, with the smallest fin density, Fig. 15(a) depicts small variations in the mean velocity profiles taken at the three spanwise locations, but Fig. 16(a) shows more variations in the fluctuation velocity amplitude up to $\pm 8\%$ at the maximum value of $\acute{u}(f_v)$. Two distinctive features of these profiles are noteworthy. First, each profile maintains a large degree of symmetry and secondly, the maximum values of $\acute{u}(f_v)$ for the three profiles shown in Fig. 16(a) are all larger than that of the bare tube as can be seen from Fig. 7, which shows a maximum value of $\acute{u}(f_v)$ near 18%. Thus, despite the observed spanwise variations in the wake characteristics of finned tube 1, the vortex shedding component $\acute{u}(f_v)$ at the three locations remains stronger than that of the bare tube. The wake characteristics for finned tube 2, Figs. 15(b) and 16(b), are generally similar to those described above for finned tube 1, except that the mean velocity profiles display substantially larger variations.

The profiles for finned tube 3, with the largest fin density, are shown in Figs. 15(c) and 16(c). The mean velocity profiles show a large variability with the spanwise distance, but all profiles consistently depict the fast recovery of the wake. In addition, although the amplitude profiles of the fluctuating velocity show slightly larger variations and less

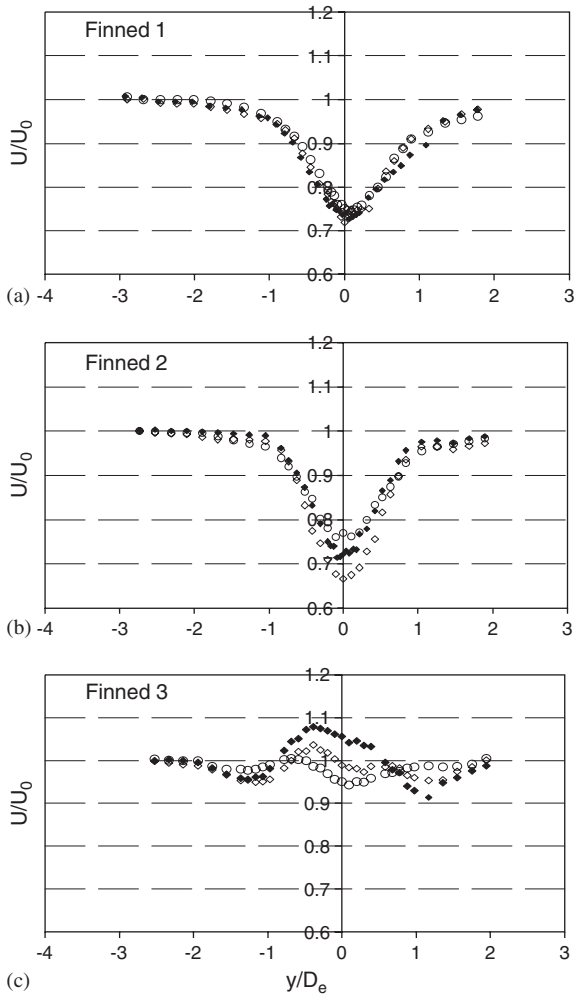

Fig. 15. Variations in mean velocity with the spanwise position z/De. All measurements were taken at $x/D_e = 5$ and low Re. (a) finned tube 1; (b) finned tube 2; (c) finned tube 3; ◆, $z/D_e = 0$; ○, $z/D_e = -2.4$; ◇, $z/D_e = 2.4$.

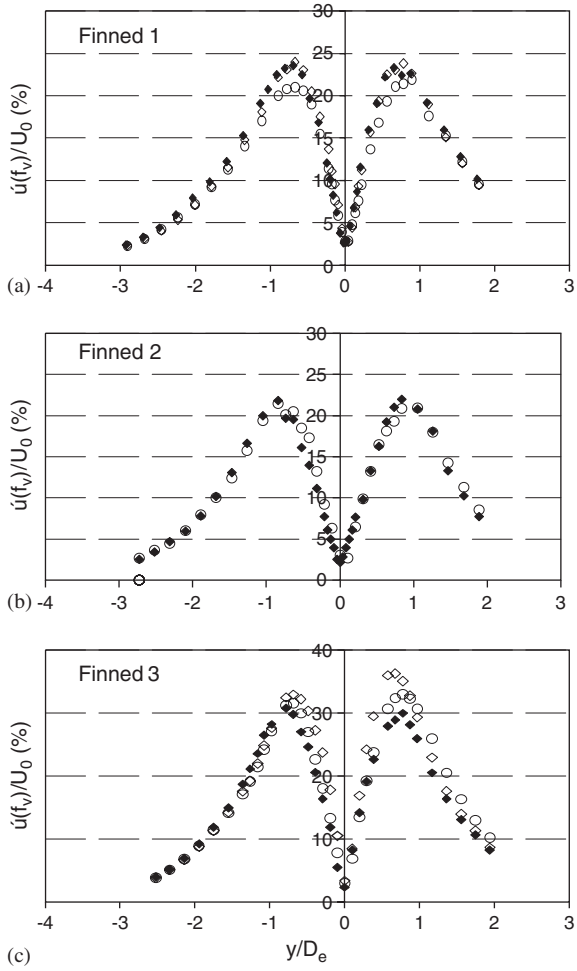

Fig. 16. Effect of the spanwise position on the profile of velocity fluctuations at the vortex shedding frequency. All measurements were taken at $x/D_e = 5$ and low Re. (a) finned tube 1; (b) finned tube 2; (c) finned tube 3; ◆, $z/D_e = 0$; ○, $z/D_e = -2.4$; ◇, $z/D_e = 2.4$.

symmetry than the other finned tubes, the lowest value of the maximum $\acute{u}(f_v)$ is about 30%, which is clearly substantially larger than those of the bare and other finned tubes. These results are all in agreement with those reported earlier in the paper.

Additional measurements were also performed for various rotation angles of the finned tubes and the results exemplified the same trends observed from the measurements at different spanwise locations. A typical example is shown in Fig. 17 for finned tube 3. The profiles were taken at $2.5D_e$ downstream of the tube and for three angles of rotation. Despite the larger differences between the three profiles, the degree of symmetry is remarkable. Here also, the three profiles show larger amplitudes of velocity fluctuation than in the case of the bare tube.

9. Conclusions

The phenomenon of vortex shedding from finned tubes has been investigated experimentally and the results are compared with those of a bare tube whose diameter is the same as the fin root diameter. Hot-wire measurements of the steady and unsteady characteristics of the wake have been performed for three tubes with segmented fins of equal height, but different density (3, 5 and 7 fins/inch). The good agreement between the bare tube results and the data

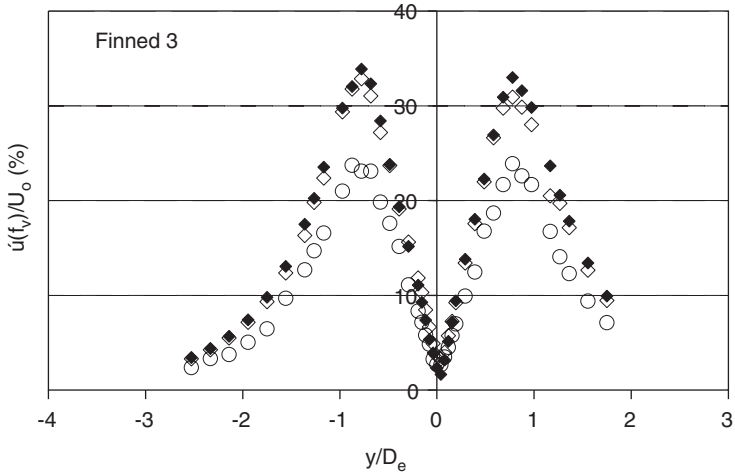

Fig. 17. Effect of rotation angle on the profile of velocity fluctuations at the vortex shedding frequency. All measurements were taken at $x/De = 2.5$ and low Re. ◆, $\phi = 0°$; ○, 120°; ◇, 240°.

available in the literature validates the experimental procedure used to investigate the finned tubes. The main findings are summarized in the following:

1. The total (streamwise) turbulence *intensity* in the wake of finned tubes is found to be comparable with that of the bare tube. However, the fins enhance velocity fluctuations at the vortex shedding frequency and its higher harmonics. For the highest fin density case, for example, the spectral peak of vortex shedding can be as much as twice that of the bare tube. Thus, the fins seem to concentrate a larger portion of the fluctuating energy into the vortex shedding component and its harmonics.
2. The use of the effective diameter to normalize the results reduces the scatter in both the Strouhal number data and the width of the wake. However, it does not seem to account for the larger wake velocity deficit observed for finned tubes 1 and 2.
3. Rotation of the present finned tubes changes the spanwise correlation length of velocity fluctuations. Apparently, this is because the fins are lined up in a wavy pattern, which changes in shape and axial location, as the tube is rotated.
4. For finned tubes 1 and 2, the correlation length measured at all rotation angles is larger than, and in some cases is twice, that of the bare tube. This finding, together with the fact that the velocity fluctuation is also enhanced by the fins, lead to the conclusion that, at least within the tested range, the addition of fins may well strengthen the process of vortex shedding, which intensifies sound generation and dynamic loading on the tube.
5. The wake of the tube with highest fin density displays several anomalies such as asymmetric profile of mean velocity, fast recovery of wake profile, and a rather short correlation length. However, the velocity fluctuation has the strongest amplitude and exhibits amplitude profiles with a large degree of symmetry. Further research is needed to be able to explain these observations and to understand the mechanism by which the fins enhance the vortex shedding process.

References

Bendat, J.S., Piersol, A.G., 1980. Engineering Applications of Correlation and Spectral Analysis. Wiley, New York.

Benney, D.J., Bergeron, R.F., 1969. A new class of nonlinear waves in parallel flows. Studies in Applied Mathematics 48, 181–204.

Blevins, R.D., 1984. Review of sound induced by vortex shedding from cylinders. Journal of Sound and Vibration 92, 455–470.

Blevins, R.D., 1994. Flow-Induced Vibration. Krieger Publishing Company, Malabar, FL.

Bloor, M.S., Gerrard, J.H., 1966. Measurements on turbulent vortices in a cylinder wake. Proceedings of the Royal Society of London, Series A: Mathematical and Physical Sciences 294, 319–342.

El Baroudi, M.Y., 1960. Measurement of two-point correlations of velocity near a circular cylinder shedding a Kaman vortex street. UTIA Technical Note No. 31, Institute of Aerophysics, University of Toronto, Canada.

Hamakawa, H., Fukano, T., Nishida, E., Aragaki, M., 2001. Vortex shedding from a circular cylinder with fin. AIAA Aeroacoustics Conference, Maastricht, Paper AIAA-2001-2215.

Jebodhsingh, D., 2002. The effect of fins on vortex shedding. Master's Thesis, Mechanical Engineering, McMaster University, Hamilton, Ontario, Canada.

Kacker, S.C., Pennington, B., Hill, R.S., 1974. Fluctuating lift coefficient for a circular cylinder in cross flow. I Mech E Journal of Mechanical Engineering Science 16 (4), 215–224.

Katinas, V., Perednis, E., Svedoscius, V., 1991. Vibrations of smooth and finned tubes in cross flows of viscous fluids with different turbulence levels. Heat Transfer—Soviet Research 23 (6), 844–851.

Kouba, J., 1986. Vortex shedding and acoustic emission in finned tube banks exposed to cross flow. in: Flow-Induced Vibrations 1986, PVP-vol. 104. ASME, New York, pp. 213–217.

Mair, W.A., Jones, P.D.F., Palmer, R.K.W., 1975. Vortex shedding from finned tubes. Journal of Sound and Vibration 39, 293–296.

Nemoto, A., Yamada, M., 1992. Flow-induced acoustic resonance caused by fin-tube bundles. Proceedings of Symposium on Flow-Induced Vibrations and Noise: vol. 4. PVP-vol. 243. ASME, New York, pp. 137–151.

Nemoto, A., Yamada, M., 1994. Flow-induced acoustic resonance in staggered tube banks. in: Flow-Induced Vibrations 1994, PVP-vol. 273. ASME PVP, Boston, pp. 273–282.

Nemoto, A., Takakuwa, A., Tsutsui, M., 1997. Flow-Induced Resonance with Various Finned Tube Banks. Proceedings of Fluid-Structure Interaction, Aeroelaciticity, Flow-Induced Vibration & Noise: vol. 2, AD 53-2. ASME, Boston, pp. 311–320.

Norberg, C., 2001. Flow around a circular cylinder: aspects of fluctuating lift. Journal of Fluids and Structures 15, 459–469.

Oengören, A., Ziada, S., 1998. A comprehensive study of vortex shedding, acoustic resonance and turbulent buffeting in normal triangular tube bundles. Journal of Fluids and Structures 12, 717–758.

Reid, D.R., Taborek, J., 1994. Selection criteria for plain and segmented finned tubes for heat recovery systems. ASME Journal of Engineering for Gas Turbines and Power 116, 406–410.

Ribeiro, J.L.D., 1992. Fluctuating lift and its spanwise correlation on a circular cylinder in a smooth and in a turbulent flow: a critical review. Journal of Wind Engineering and Industrial Aerodynamics 40, 179–198.

Robinson, J.L., 1974. The inviscid nonlinear instability of parallel shear flows. Journal of Fluid Mechanics 63, 723–752.

Stansby, P.K., 1974. The effects of end plates on the base pressure coefficient of a circular cylinder. Aeronautical Journal 78, 36–37.

Stuart, J.T., 1971. Nonlinear stability theory. Annual Review of Fluid Mechanics 3, 347–370.

Szepessy, S., 1994. On the spanwise correlation of vortex shedding from a circular cylinder at high Reynolds number. Physics of Fluids 6 (7), 2406–2416.

Szepessy, S., Bearman, P.W., 1992. Aspect ratio and end plate effects on vortex shedding from a circular cylinder. Journal of Fluid Mechanics 234, 191–217.

Weaver, D.S., 1993. Vortex shedding and acoustic resonance in heat exchanger tube arrays. In: Technology for the '90s. ASME, New York, pp. 777–810.

Zdravkovich, M.M., 1981. Review and classification of various aerodynamic and hydrodynamic means for suppressing vortex shedding. Journal of Wind Engineering and Industrial Aerodynamics 7, 145–189.

Ziada, S., Oengören, A., 1992. Vorticity shedding and acoustic resonance in an in-line tube bundle; Part I: vorticity shedding. Journal of Fluids and Structures 6, 271–292.

Ziada, S., Oengören, A., 2000. Flow periodicity and acoustic resonance in parallel triangle tube bundles. Journal of Fluids and Structures 14, 197–219.

Ziada, S., Rockwell, D., 1982. Generation of higher harmonics in a self-oscillating mixing layer-wedge system. AIAA Journal 20, 196–202.